

Received November 21, 2019, accepted December 3, 2019, date of publication December 6, 2019, date of current version December 23, 2019.

Digital Object Identifier 10.1109/ACCESS.2019.2958117

# Rate-Energy Outage Analysis of MISO SWIPT With Multiple Energy Harvesting Sensors

MINCHUL JU<sup>1</sup>, (Member, IEEE), AND HONG-CHUAN YANG<sup>2</sup>, (Senior Member, IEEE)

<sup>1</sup>School of Electrical Engineering, Kookmin University, Seoul 02707, South Korea

<sup>2</sup>Department of Electrical and Computer Engineering, University of Victoria, Victoria, BC V8P 5C2, Canada

Corresponding author: MinChul Ju (mcju@kookmin.ac.kr)

This work was supported by the National Research Foundation of Korea (NRF) Grant through by the Korea Government (MSIT) under Grant NRF-2019R1F1A1062720.

**ABSTRACT** We study a multi-input-single-output (MISO) transmission system consisting of a multi-antenna basestation (BS) and a single-antenna user in the presence of multiple single-antenna radio frequency (RF) energy harvesting (EH) sensor nodes, where the user decodes information and multiple EH sensor nodes accumulate energy through the received signal from the BS. The sensor nodes coordinate their transmissions to perform virtual MISO beamforming, which requires sufficient individual and sum transmission power across multiple sensor nodes. For this reason, we consider simultaneously both the individual and sum EH constraints for SWIPT networks. Specifically, under both the individual and sum EH constraints, we propose beam selection of random unitary beamforming to maximize the transmission rate of the MISO system. Then we derive the exact rate-energy outage probability in closed-form for the system with identical average value of harvested energy across all sensor nodes and the exact probability in recursive form for the system with distinct average value of harvested energy at each sensor node. Numerical results confirm that the analyses are exact and the outage performance improves as the number of antennas at the BS increases and/or as the average received power at the user and sensor nodes increases.


**INDEX TERMS** Beam selection, individual/sum energy harvesting (EH) constraint, multiple EH sensor nodes, multi-input-single-output (MISO) system, random unitary beamforming.

## I. INTRODUCTION

Energy harvesting (EH) technologies supply energy to devices by wireless energy transfer [1]–[7]. Radio frequency (RF) radiation is used to recharge the batteries of wireless devices, instead of replacing batteries or charging from alternating current (AC) power supply. Since RF radiation can convey information as well as energy at the same time, simultaneous wireless information and power transfer (SWIPT) has received a great attention in the research community [8]–[15]. In fact, SWIPT has been considered as a promising candidate to extend the lifetime of wireless networks such as sensor networks and cellular networks. In general, there are two scenarios in SWIPT systems: 1) a terminal can be either an information decoder or an energy harvester [9]–[13]; and 2) a terminal acts as both an information decoder and an energy harvester at the same time [14], [15]. Apparently, the first

scenario allows simpler hardware implementation, and will be the focus of this work.

In the literature, the rate-energy region (or capacity-energy region) has been defined to characterize all the achievable rate and harvested energy combinations for SWIPT networks [8]–[12]. In these works, the rate-energy region satisfied two constraints, i.e., the successful information decoding at the decoder and sufficient energy harvesting at the harvester. When there exist multiple energy harvesters in the networks, we can consider two different EH constraints: the harvested energy by each harvester must be greater than a certain threshold, which is denoted by the individual EH constraint; and the sum of harvested energy by all the harvesters must be greater than another threshold, which is denoted by the sum EH constraint [16]–[19]. Liu *et al.* considered two different problems: the first was to maximize the secrecy rate for the information receiver under the individual EH constraint, and the second was to maximize the sum-energy at energy harvesters under the secrecy rate constraint [16]. Xu *et al.* aimed to maximize the sum-energy at energy harvesters under the

The associate editor coordinating the review of this manuscript and approving it for publication was Ding Xu .

given minimum signal-to-interference-and-noise ratio constraint [17]. Ho and Zhang considered the throughput maximization problem with full side information under the sum EH constraint [18]. To the best of our knowledge, no previous work has considered the two EH constraints simultaneously. In a certain scenario, energy harvesters need to satisfy both the individual and sum EH constraints at the same time. For example, in multi-hop sensor networks, sensor nodes need to harvest energy for possible next hop transmissions. During the transmission phase, the sensor nodes coordinate their transmissions to perform virtual multi-input-single-output (MISO)/multi-input-multi-output (MIMO) beamforming for the maximum signal-to-noise ratio (SNR) at the destination. Such virtual MISO/MIMO transmission demands sufficient individual and sum transmission power [20]–[24]. In this phase, the individual EH constraint can guarantee sufficient individual transmission power, and the sum EH constraint can guarantee sufficient sum transmission power. For this reason, it is necessary to simultaneously consider both the individual and sum EH constraints for SWIPT networks with multiple energy harvesters.

Among the available transmission strategies to exploit multiple antennas, random unitary beamforming has been widely used in the classical MISO/MIMO systems. Although random beams are not perfectly matched to the channel, random beamforming can achieve full diversity order with low complexity and very low feedback signalling overhead compared with the conventional focused beamforming [25]–[28]. Recently, conventional SWIPT techniques have been combined with random unitary beamforming [29], [30]. Wu *et al.* considered a random unitary beamforming-based cooperative beam selection to improve the performance of SWIPT systems with a single EH node [29], and they also considered cooperative beam selection for the cognitive MISO/MIMO system without any EH node [30]. As a special case of random unitary beamforming, transmit antenna selection in SWIPT networks has also been recently studied in many works [31]–[33]. Han *et al.* analyzed the outage performance of downlink non-orthogonal multiple access (NOMA) SWIPT relaying networks with transmit antennas selection [31]. Ye *et al.* analyzed the outage performance of a cooperative system where the wireless-powered relays had finite energy storage and applied transmit antenna selection over Nakagami- $m$  fading channels [32]. Orikumhi *et al.* investigated the inter-relay interference of SWIPT MIMO virtual full duplex relaying with transmit antenna selection at the relay [33]. To the best of our knowledge, however, there has been no work on random unitary beamforming/transmit antenna selection in SWIPT networks with multiple EH nodes and its rate-energy outage performance analysis.

In this work, we consider a MISO transmission system consisting of a base-station (BS) and a user with multiple EH sensor nodes, where the user decodes information and multiple sensor nodes accumulate energy through the received signals from the BS. The system model can also apply to a multi-user system where one user decodes information and

other users harvest energy through the received signals from the BS. Specifically, the contributions of this paper can be summarized as follows. We propose a beam selection scheme for random unitary beamforming to maximize the transmission rate of the MISO system under both the individual and sum EH constraints at multiple EH sensor nodes. Then we derive the exact rate-energy outage probability in closed-form for the system with identical average value of harvested energy across all sensor nodes and the exact probability in recursive form for the system with distinct average value of harvested energy at each sensor node. Finally, we obtain rate-energy outage probabilities for two special cases: a system under only the individual EH constraint and a system under only the sum EH constraint. Numerical results confirm that the analyses are exact and the outage performance improves as the number of antennas at the BS increases and/or as the average received power at the user and sensor nodes increases.

In particular, our work is different from [34]. The authors of [34] considered the single-antenna BS without beamforming, single-input-single-output (SISO) multi-hop relaying among secondary users, and joint iterative optimal time and power allocation algorithm, whereas we consider the multi-antenna BS, MISO/MIMO transmission among energy harvesting (EH) sensor nodes, and beam selection of random unitary beamforming and analyze the exact rate-energy outage probability.

The remainder of this paper is organized as follows. In Section II, we describe the system model. In Section III, we propose beam selection of random unitary beamforming to maximize the transmission rate of the MISO transmission system. In Section IV, we derive rate-energy outage probabilities. In Section V, we present numerical results. Finally, conclusions are drawn in Section VI.

## II. SYSTEM MODEL

We consider a MISO transmission with energy transfer system depicted in Fig. 1, which consists of one  $L$ -antenna BS, one single-antenna user, and multiple single-antenna EH sensor nodes. The BS transmits information to the user and simultaneously charges EH sensor nodes.<sup>1</sup> The complex

<sup>1</sup>Since our system supports WIT (wireless information transfer) and WPT (wireless power transfer) simultaneously, it can be classified as a SWIPT system [9].

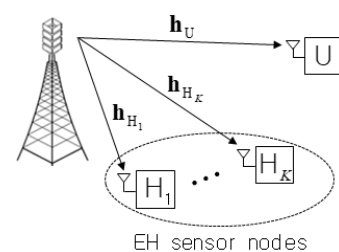


**FIGURE 1.** System model for a MISO transmission system consisting of a multi-antenna BS and a single-antenna user in the presence of multiple single-antenna EH sensor nodes.

channel vector from the BS to the user is denoted by  $h_U = [h_{1,U}, h_{2,U}, \dots, h_{L,U}]^T$ , and the complex channel vector from the BS to the  $k$ -th EH sensor node is denoted by  $h_{H_k} = [h_{1,H_k}, h_{2,H_k}, \dots, h_{L,H_k}]^T$ . It is assumed that all the channel coefficients are fixed during a channel coherence time, and they are modeled as  $h_{l,U} \sim \mathcal{CN}(0, \Omega_U)$  and  $h_{l,H_k} \sim \mathcal{CN}(0, \Omega_{H_k})$ , where  $h \sim \mathcal{CN}(m, \Omega)$  indicates that  $h$  is a circularly symmetric complex-valued Gaussian random variable with mean  $m$  and variance  $\Omega$ .

The BS serves the user using one out of  $L$  orthonormal beams, which are generated from an isotropic distribution [25]. Let  $\mathcal{W} = \{w_1, w_2, \dots, w_L\}$  denote the set of orthonormal beamforming vectors, where  $w_l = [w_{l,1}, w_{l,2}, \dots, w_{l,L}]^T$  with  $\sum_{i=1}^L |w_{l,i}|^2 = 1$  and  $\sum_{i=1}^L w_{l,i} w_{j,i}^* = 0$  for  $l, j = 1, \dots, L$  and  $j \neq l$ , which is assumed to be known to the user. When the BS transmits its signal using the  $l$ -th beamforming vector  $w_l$ , the received signal  $r_l$  at the user is given by

$$r_l = \sqrt{P_{BS}} h_U^T w_l s + v, \tag{1}$$

where  $P_{BS}$  is the transmission power at the BS,  $s$  is the transmitted symbol from the BS with unit power, and  $v$  is the additive white Gaussian noise (AWGN) at the user with  $v \sim \mathcal{CN}(0, 1)$ . We let  $\gamma_{l,U}$  denote the instantaneous SNR at the user when the BS transmits its signal using  $w_l$ , where  $\gamma_{l,U} = P_{BS} |h_U^T w_l|^2 = P_{BS} \left| \sum_{i=1}^L w_{l,i} h_{i,U} \right|^2$ . Note that  $\gamma_{l,U}$  is exponentially distributed with mean  $\bar{\gamma}_{l,U} = P_{BS} \Omega_U$  because  $\sum_{i=1}^L w_{l,i} h_{i,U} \sim \mathcal{CN}(0, \Omega_U)$ . Also, when the BS transmits its signal using  $w_l$ , the received power  $\mathcal{P}_{l,k}$  at the  $k$ -th EH sensor node is given by

$$\mathcal{P}_{l,k} = P_{BS} |h_{H_k}^T w_l|^2 = P_{BS} \left| \sum_{i=1}^L w_{l,i} h_{i,H_k} \right|^2. \tag{2}$$

Note that  $\mathcal{P}_{l,k}$  is exponentially distributed with mean  $\bar{\mathcal{P}}_{l,k} = P_{BS} \Omega_{H_k}$ . Since  $w_l$  and  $w_j$  are orthonormal beamforming vectors, it can be shown for  $l \neq j$  that two complex Gaussian random variables  $h_U^T w_l = \sum_{i=1}^L w_{l,i} h_{i,U}$  and  $h_U^T w_j = \sum_{i=1}^L w_{j,i} h_{i,U}$  are independent, which results in the independence between  $\gamma_{l,U}$  and  $\gamma_{j,U}$ . Also, it can be shown that two complex Gaussian random variables  $h_{H_k}^T w_l = \sum_{i=1}^L w_{l,i} h_{i,H_k}$  and  $h_{H_k}^T w_j = \sum_{i=1}^L w_{j,i} h_{i,H_k}$  are independent, which results in the independence between  $\mathcal{P}_{l,k}$  and  $\mathcal{P}_{j,k}$ .

### III. BEAM SELECTION TO MAXIMIZE TRANSMISSION RATE OF MISO SYSTEM

In this section, we propose a beam selection scheme for random unitary beamforming to maximize the transmission rate of the MISO system while satisfying both the individual and sum EH constraints of multiple EH sensor nodes.

#### A. INDIVIDUAL AND SUM EH CONSTRAINTS OF MULTIPLE ENERGY HARVESTERS

In wireless sensor networks, multiple low cost and low power sensor nodes gather data and collaborate to forward sensed data to sink(s). Replacing batteries regularly of

numerous sensor nodes costs a lot, and many researchers have investigated EH sensor nodes. The EH sensor nodes have two different phases: energy harvesting and transmission phases. During the EH phase, sensor nodes need to harvest energy for possible next hop transmissions; and during the information transmission phase, the sensor nodes could coordinate their transmissions to perform virtual MISO/MIMO beamforming for the coverage range extension and energy efficiency enhancement. Such virtual MISO/MIMO transmission requires sufficient transmission power, where MISO/MIMO optimization problems are subject to both individual and sum transmission power requirements [20]–[24]. In order to satisfy the two transmission power requirements of the information transmission phase, it is necessary to harvest sufficient energy during the EH phase. Specifically, the sufficient individual transmission power can be guaranteed by the individual EH constraint, and the sufficient sum transmission power can be guaranteed by the sum EH constraint. For this reason, we consider simultaneously both the individual and sum EH constraints for SWIPT networks with multiple EH sensor nodes.

We let  $\mathcal{E}_{l,k}$  denote the harvested energy of the  $k$ -th EH sensor node over a channel coherence time  $T_c$  when the  $l$ -th beamforming vector  $w_l$  is selected, and it is given by

$$\mathcal{E}_{l,k} = \eta_k \mathcal{P}_{l,k} T_c, \tag{3}$$

where  $\eta_k$  is the energy conversion efficiency at the  $k$ -th EH sensor node with  $0 \leq \eta_k \leq 1$ , whose value depends on the energy conversion circuitry. Note that  $\mathcal{E}_{l,k}$  is exponentially distributed with mean  $\bar{\mathcal{E}}_{l,k} = \eta_k \bar{\mathcal{P}}_{l,k} T_c$ . To satisfy the individual EH constraint,  $\mathcal{E}_{l,k}$  must be greater than or equal to a target individual harvested energy  $E_k$  in joule, i.e.,  $\mathcal{E}_{l,k} \geq E_k$  for  $k = 1, \dots, K$ . Also, to satisfy the sum EH constraint,  $\sum_{k=1}^K \mathcal{E}_{l,k}$  must be greater than or equal to a target sum harvested energy  $E_{sum}$  in joule, i.e.,  $\sum_{k=1}^K \mathcal{E}_{l,k} \geq E_{sum}$ . We let  $\mathcal{D}_{EH}$  denote the set of indices for those beams that satisfy both the individual and sum EH constraints and given by

$$\mathcal{D}_{EH} = \left\{ l \in \{1, \dots, L\} : \mathcal{E}_{l,1} \geq E_1, \mathcal{E}_{l,2} \geq E_2, \dots, \right. \\ \left. \mathcal{E}_{l,K} \geq E_K, \sum_{k=1}^K \mathcal{E}_{l,k} \geq E_{sum} \right\}. \tag{4}$$

Note that if the set  $\mathcal{D}_{EH}$  has no element, i.e.  $\mathcal{D}_{EH} = \emptyset$ , then no beamforming vector satisfies both the individual and sum EH constraints.

#### B. OPTIMUM BEAMFORMING VECTOR

In this work, we consider random unitary beamforming, which is different from conventional optimum beamforming. Random unitary beamforming is generally adopted in scenarios where the amount of feedback available at the BS is limited. Specifically, random unitary beams are predetermined and are not perfectly matched to the given channel, which results in low computational complexity than conventional optimum beamforming [25]–[28]. For a given channel,

random unitary beamforming selects one of predetermined beams with the partial channel state information (CSI), whereas conventional optimum beamforming calculate optimum beams with the full CSI [35].

The optimum beamforming vector over each channel coherence time should be chosen such that the achievable rate at the user must be maximized under both the individual and sum EH constraints at EH sensor nodes. Specifically, when the  $l$ -th beamforming vector  $w_l$  is selected, the achievable rate  $I_l$  at the user is given by [35, eq. (6.22)]

$$I_l = \log_2(1 + \gamma_{l,U}). \tag{5}$$

As such, the index  $\hat{l}$  of the selected beam can be determined as follows

$$\hat{l} = \arg \max_{l \in \mathcal{D}_{EH}} I_l. \tag{6}$$

If none of beamforming vectors satisfies both the individual and sum EH constraints with  $\mathcal{D}_{EH} = \emptyset$ , then it is possible that none is selected, i.e.,  $\hat{l} = -\infty$ . The proposed beam selection can be implemented as follows. At the beginning of every channel coherence time, the BS collects the required CSI. With the CSI, the achievable rates  $\{I_l : l = 1, \dots, L\}$  and the harvested energy  $\{\mathcal{E}_{l,k} : l = 1, \dots, L, k = 1, \dots, K\}$  are calculated at the BS. Then the BS transmits the signal using the selected beam  $w_{\hat{l}}$  to the user and EH sensor nodes for the channel coherence time. When the channels are not reciprocal, the CSI signalling strategy is composed of two phases. Specifically, in the first phase, the BS broadcasts sequentially a pilot signal using  $w_l$  to the user and EH sensor nodes for  $l = 1, \dots, L$ . In the second phase, the user and each EH sensor node feed back the CSI to the BS. On the other hand, when the channels are reciprocal, the CSI signalling becomes much simpler: the user and each EH sensor node transmit sequentially their pilot signals to the BS, and the BS obtains the CSI.

#### IV. RATE-ENERGY OUTAGE PROBABILITY ANALYSIS

In this section, we derive the exact rate-energy outage probability of the MISO system with random unitary beamforming and best beam selection under both the individual and sum EH constraints. Then we provide rate-energy outage probabilities for two special cases.

##### A. GENERAL CASE

The MISO transmission system with one user and multiple EH sensor nodes is considered to be in rate-energy outage either if the user fails to decode information, i.e.,  $I_{\hat{l}}$  is less than a particular threshold  $R$ , or if the individual EH constraint or sum EH constraint is not satisfied. Therefore, there is no priority among the user and sensor nodes. We let  $P_{out}^{BS}(R, E)$  denote the rate-energy outage probability of the MISO system with random unitary beamforming and best beam selection under the individual and sum EH constraints, where  $E = [E_{sum}, E_1, \dots, E_K]$ . The rate-energy outage

probability  $P_{out}^{BS}(R, E)$  is calculated as

$$\begin{aligned} P_{out}^{BS}(R, E) &= Pr \left[ \max_{l \in \mathcal{D}_{EH}} I_l < R \right] \\ &= Pr \left[ \max_{l \in \mathcal{D}_{EH}} \gamma_{l,U} < T_r \right], \end{aligned} \tag{7}$$

where  $T_r = 2^R - 1$ . Note that the selection rule in (6), which maximizes the achievable rate under the two EH constraints, also minimizes the rate-energy outage probability in (7). As can be seen in (7) with (4), the individual EH constraints,  $\{\mathcal{E}_{l,k} \geq E_k\}_{k=1}^K$ , and the sum EH constraint,  $\sum_{k=1}^K \mathcal{E}_{l,k} \geq E_{sum}$ , are highly correlated each other, which makes the mathematical derivation difficult. In the following theorem, we present the rate-energy outage probability in simplified form.

*Theorem 1:* The rate-energy outage probability  $P_{out}^{BS}(R, E)$  of the MISO system with random unitary beamforming and best beam selection under both the individual and sum EH constraints is given by

$$\begin{aligned} P_{out}^{BS}(R, E) &= \prod_{l=1}^L \left( 1 - \exp \left( -\frac{T_r}{\gamma_{l,U}} \right) \right. \\ &\quad \left. \times \Upsilon_{l,K}(E_{sum}, \{E_k\}_{k=1}^K; \{\bar{\mathcal{E}}_{l,k}\}_{k=1}^K) \right), \end{aligned} \tag{8}$$

where

$$\begin{aligned} \Upsilon_{l,K}(E_{sum}, \{E_k\}_{k=1}^K; \{\bar{\mathcal{E}}_{l,k}\}_{k=1}^K) \\ = Pr \left[ \mathcal{E}_{l,1} \geq E_1, \dots, \mathcal{E}_{l,K} \geq E_K, \sum_{k=1}^K \mathcal{E}_{l,k} \geq E_{sum} \right], \end{aligned} \tag{9}$$

with average value  $\bar{\mathcal{E}}_{l,k}$  of harvested energy at the  $k$ -th EH sensor node.

*Proof:* See Appendix A. □

In the following lemmas, we calculate the probability  $\Upsilon_{l,K}(E_{sum}, \{E_k\}_{k=1}^K; \{\bar{\mathcal{E}}_{l,k}\}_{k=1}^K)$  for three cases: 1) when  $\sum_{k=1}^K E_k \geq E_{sum}$ ; 2) when  $\sum_{k=1}^K E_k < E_{sum}$  and all the average values of harvested energy  $\{\bar{\mathcal{E}}_{l,k}\}_{k=1}^K$  are distinct; and 3) when  $\sum_{k=1}^K E_k < E_{sum}$  and all the average values of harvested energy  $\{\bar{\mathcal{E}}_{l,k}\}_{k=1}^K$  are identical.<sup>2</sup>

*Lemma 1:* When  $\sum_{k=1}^K E_k \geq E_{sum}$ , the probability  $\Upsilon_{l,K}(E_{sum}, \{E_k\}_{k=1}^K; \{\bar{\mathcal{E}}_{l,k}\}_{k=1}^K)$  is given by

$$\Upsilon_{l,K}(E_{sum}, \{E_k\}_{k=1}^K; \{\bar{\mathcal{E}}_{l,k}\}_{k=1}^K) = \prod_{k=1}^K \exp \left( -\frac{E_k}{\bar{\mathcal{E}}_{l,k}} \right). \tag{10}$$

*Proof:* If  $\mathcal{E}_{l,k} \geq E_k$  for  $k = 1, \dots, K$ , it is always true that  $\sum_{k=1}^K \mathcal{E}_{l,k} \geq E_{sum}$ . Therefore,

<sup>2</sup>In this work, although we do not present the probability  $\Upsilon_{l,K}(E_{sum}, \{E_k\}_{k=1}^K; \{\bar{\mathcal{E}}_{l,k}\}_{k=1}^K)$  when  $\sum_{k=1}^K E_k < E_{sum}$  and some average values of harvested energy are identical, one can easily derive the result by taking steps similar to those used in Appendixes B and C. Due to the space limit, we present the results only when all the average values are distinct or identical.



$\Upsilon_{l,K}(E_{sum}, \{E_k\}_{k=1}^K; \{\bar{\mathcal{E}}_{l,k}\}_{k=1}^K)$  of (9) can be simplified to

$$\begin{aligned} & \Upsilon_{l,K}(E_{sum}, \{E_k\}_{k=1}^K; \{\bar{\mathcal{E}}_{l,k}\}_{k=1}^K) \\ &= \Pr[\mathcal{E}_{l,1} \geq E_1, \mathcal{E}_{l,2} \geq E_2, \dots, \mathcal{E}_{l,K} \geq E_K] \\ &= \prod_{k=1}^K \Pr[\mathcal{E}_{l,k} \geq E_k]. \end{aligned} \quad (11)$$

Since  $\{\mathcal{E}_{l,k}\}_{k=1}^K$  are exponentially distributed with mean  $\{\bar{\mathcal{E}}_{l,k}\}_{k=1}^K$ , the probability  $\Upsilon_{l,K}(E_{sum}, \{E_k\}_{k=1}^K; \{\bar{\mathcal{E}}_{l,k}\}_{k=1}^K)$  is calculated as (10).  $\square$

*Lemma 2:* When  $\sum_{k=1}^K E_k < E_{sum}$  and all the average values of harvested energy  $\{\bar{\mathcal{E}}_{l,k}\}_{k=1}^K$  are distinct, i.e.,  $\bar{\mathcal{E}}_{l,i} \neq \bar{\mathcal{E}}_{l,j}$  for  $i \neq j$  with  $i, j = 1, \dots, K$ , the probability  $\Upsilon_{l,K}(E_{sum}, \{E_k\}_{k=1}^K; \{\bar{\mathcal{E}}_{l,k}\}_{k=1}^K)$  is given in recursive form for a positive integer  $K$ , i.e.,  $K \geq 2$ , as follows:

$$\begin{aligned} & \Upsilon_{l,K}(E_{sum}, \{E_k\}_{k=1}^K; \{\bar{\mathcal{E}}_{l,k}\}_{k=1}^K) \\ &= \Upsilon_{l,K-1}(E_{sum} - E_K, \{E_k\}_{k=1}^{K-1}; \{\bar{\mathcal{E}}_{l,k}\}_{k=1}^{K-1}) \\ & \quad \times \exp\left(-\frac{E_K}{\bar{\mathcal{E}}_{l,K}}\right) \\ & \quad + \sum_{j=1}^K \frac{\bar{\mathcal{E}}_{l,j}^{K-2} \bar{\mathcal{E}}_{l,K}}{\prod_{i=1, i \neq j}^K (\bar{\mathcal{E}}_{l,i} - \bar{\mathcal{E}}_{l,j})} \\ & \quad \times \exp\left(-\sum_{i=1, i \neq j}^K \frac{E_i}{\bar{\mathcal{E}}_{l,i}} - \frac{E_{sum} - \sum_{i=1, i \neq j}^K E_i}{\bar{\mathcal{E}}_{l,j}}\right), \end{aligned} \quad (12)$$

with the initial value  $\Upsilon_{l,1}(E_{sum}, E_1; \bar{\mathcal{E}}_{l,1}) = \exp(-E_{sum}/\bar{\mathcal{E}}_{l,1})$ .

*Proof:* See Appendix B.  $\square$

*Lemma 3:* When  $\sum_{k=1}^K E_k < E_{sum}$  and all the average values of harvested energy  $\{\bar{\mathcal{E}}_{l,k}\}_{k=1}^K$  are identical, i.e.,  $\bar{\mathcal{E}}_{l,k} = \bar{\mathcal{E}}_l$  for  $k = 1, \dots, K$ , the probability  $\Upsilon_{l,K}(E_{sum}, \{E_k\}_{k=1}^K; \{\bar{\mathcal{E}}_{l,k}\}_{k=1}^K)$  is given in closed-form as follows:

$$\begin{aligned} & \Upsilon_{l,K}(E_{sum}, \{E_k\}_{k=1}^K; \{\bar{\mathcal{E}}_{l,k}\}_{k=1}^K) \\ &= \frac{1}{(K-1)!} \exp\left(-\frac{\sum_{k=1}^K E_k}{\bar{\mathcal{E}}_l}\right) \Gamma\left(K, \frac{E_{sum} - \sum_{k=1}^K E_k}{\bar{\mathcal{E}}_l}\right), \end{aligned} \quad (13)$$

where  $\Gamma(K, x)$  denotes the standard upper incomplete Gamma function [36], where  $\Gamma(K, x) = \int_x^\infty t^{K-1} \exp(-t) dt$ .

*Proof:* See Appendix C.  $\square$

Note that the probability  $\Upsilon_{l,K}(E_{sum}, \{E_k\}_{k=1}^K; \{\bar{\mathcal{E}}_{l,k}\}_{k=1}^K)$  of (9) is given in closed form when  $\sum_{k=1}^K E_k \geq E_{sum}$  or when  $\sum_{k=1}^K E_k < E_{sum}$  and all the average values of harvested energy are identical; and it is given in recursive form when  $\sum_{k=1}^K E_k < E_{sum}$  and all the average values of harvested energy are distinct.

## 1) ANOTHER EXPRESSION OF RATE-ENERGY OUTAGE

From (A.1) with (A.3), the rate-energy outage probability of can be given in another form as

$$P_{out}^{BS}(R, E) = \prod_{l=1}^L \left(1 - \Pr[\gamma_{l,U} \geq T_r] \Pr[l \in \mathcal{D}_{EH}]\right). \quad (14)$$

Then we can show that the above equation can be easily reduced to the conventional rate outage probability and energy outage probability. Specifically, setting  $E_1 = E_2 = \dots = E_K = E_{sum} = 0$  yields the rate outage probability  $P_{R,out}^{BS}(R)$ , and setting  $R = 0$ , or equivalently  $T_r = 0$ , yields the energy outage probability  $P_{E,out}^{BS}(E)$  as

$$P_{R,out}^{BS}(R) = \prod_{l=1}^L \left(1 - \exp\left(-\frac{T_r}{\bar{\gamma}_{l,U}}\right)\right) \quad (15)$$

$$P_{E,out}^{BS}(E) = \prod_{l=1}^L \left(1 - \Upsilon_{l,K}(E_{sum}, \{E_k\}_{k=1}^K; \{\bar{\mathcal{E}}_{l,k}\}_{k=1}^K)\right). \quad (16)$$

## B. TWO SPECIAL CASES

*Corollary 1 (Under Only Individual EH Constraint):* When there exists only the individual EH constraint of the MISO system with multiple EH sensor nodes, the rate-energy outage probability  $P_{out}^{BS}(R, E)$  of (8) reduces to

$$P_{out}^{BS}(R, E) = \prod_{l=1}^L \left(1 - \exp\left(-\frac{T_r}{\bar{\gamma}_{l,U}} - \sum_{k=1}^K \frac{E_k}{\bar{\mathcal{E}}_{l,k}}\right)\right). \quad (17)$$

*Proof:* When there exists only the individual EH constraint without the sum EH constraint, it is obvious that  $E_{sum} = 0$  and is equivalent to  $\sum_{k=1}^K E_k \geq E_{sum}$ . This results in  $\Upsilon_{l,K}(E_{sum}, \{E_k\}_{k=1}^K; \{\bar{\mathcal{E}}_{l,k}\}_{k=1}^K) = \exp(-\sum_{k=1}^K E_k/\bar{\mathcal{E}}_{l,k})$ , which in turn is substituted into (8) yields (17).  $\square$

*Corollary 2 (Under Only Sum EH Constraint):* When there exists only the sum EH constraint of the MISO system with multiple EH sensor nodes, the rate-energy outage probability  $P_{out}^{BS}(R, E)$  of (8) reduces to

$$\begin{aligned} P_{out}^{BS}(R, E) &= \prod_{l=1}^L \left(1 - \exp\left(-\frac{T_r}{\bar{\gamma}_{l,U}}\right) \right. \\ & \quad \times \left(1 - \sum_{i_1=1}^{\varrho(\mathcal{B})} \sum_{i_2=1}^{\tau_{i_1}(\mathcal{B})} \chi_{i_1, i_2}(\mathcal{B}) \right. \\ & \quad \left. \left. \times \left(1 - \frac{\Gamma(i_2, E_{sum}/\bar{\mathcal{E}}_{l, (i_1)})}{(i_2 - 1)!}\right)\right)\right), \end{aligned} \quad (18)$$

where  $\mathcal{B} = \text{diag}[\bar{\mathcal{E}}_{l,1}, \bar{\mathcal{E}}_{l,2}, \dots, \bar{\mathcal{E}}_{l,K}]$ ,  $\varrho(\mathcal{B})$  is the number of distinct diagonal elements of  $\mathcal{B}$ ,  $\bar{\mathcal{E}}_{l, (1)} > \bar{\mathcal{E}}_{l, (2)} > \dots > \bar{\mathcal{E}}_{l, (\varrho(\mathcal{B}))}$  are the distinct diagonal elements in decreasing order,  $\tau_{i_1}(\mathcal{B})$  is the multiplicity of  $\bar{\mathcal{E}}_{l, (i_1)}$ , and  $\chi_{i_1, i_2}(\mathcal{B})$  is the  $(i_1, i_2)$ -th characteristic coefficient of  $\mathcal{B}$ .

*Proof:* When there exists only the sum EH constraint without the individual EH constraint, it is obvious that  $E_k = 0$  for  $k = 1, \dots, K$ , and  $\sum_{k=1}^K E_k < E_{sum}$ . Since  $\Upsilon_{l,K}(E_{sum}, \{E_k\}_{k=1}^K; \{\bar{\mathcal{E}}_{l,k}\}_{k=1}^K)$  of (12) is given in recursive form, we take another approach to derive a closed-form expression. Using [37, eq. (29)], the cumulative distribution function (CDF)  $F_{\sum_{k=1}^K \mathcal{E}_{l,k}}(y)$  of the sum of harvested

energy  $\sum_{k=1}^K \mathcal{E}_{l,k}$  is given by

$$F_{\sum_{k=1}^K \mathcal{E}_{l,k}}(y) = \sum_{i_1=1}^{\varrho(\mathcal{B})} \sum_{i_2=1}^{\tau_{i_1}(\mathcal{B})} \chi_{i_1, i_2}(\mathcal{B}) \times \left( 1 - \frac{\Gamma(i_2, y/\bar{\mathcal{E}}_{l, (i_1)})}{(i_2 - 1)!} \right). \quad (19)$$

Note that  $\Psi_{l,K}(E) = 1 - \Pr[\sum_{k=1}^K \mathcal{E}_{l,k} < E_{sum}] = 1 - F_{\sum_{k=1}^K \mathcal{E}_{l,k}}(E_{sum})$ , which is substituted into (8) yields (18).  $\square$

**V. NUMERICAL RESULTS**

In this section, we verify the accuracy of the obtained rate-energy outage probability results by comparing our analytical results with computer based Monte Carlo simulations.

**A. RATE-ENERGY OUTAGE PROBABILITY OF MISO SYSTEM WITH RANDOM UNITARY BEAMFORMING AND BEST BEAM SELECTION UNDER BOTH INDIVIDUAL AND SUM EH CONSTRAINTS**

In this subsection, we check the accuracy of the obtained rate-energy outage probability of (8) with (10)–(13) for the MISO system under both the individual and sum EH constraints. Fig. 2 shows the rate-energy outage probability against  $\bar{\gamma}$  of the MISO system with random unitary beamforming and best beam selection in the presence of three EH sensor nodes under both the individual and sum EH constraints when  $\sum_{k=1}^K E_k \geq E_{sum}$ , where we set  $L = 1, 2, 3, 4$ ,  $\bar{\gamma}_{l,U} = \bar{\gamma}$  and  $\bar{\mathcal{E}}_{l,k} = \bar{\gamma}/10$ ,  $R = 3$  bps/Hz,  $E_k = 2$  and  $E_{sum} = 6$  for  $l = 1, \dots, L$  and  $k = 1, 2, 3$ . For this case, the result is given in closed form of (8) with (10). Fig. 3 shows the rate-energy outage probability against  $\bar{\gamma}$  of the MISO system with random unitary beamforming and best beam selection in the

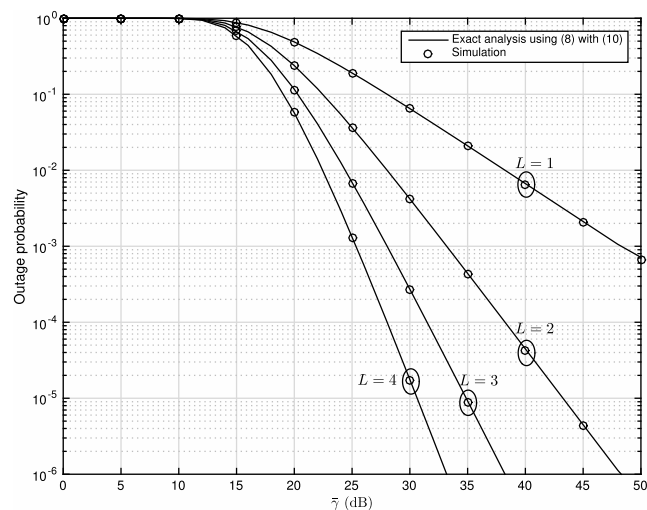


**FIGURE 2.** Rate-energy outage probability against  $\bar{\gamma}$  of the MISO system with random unitary beamforming and best beam selection in the presence of three EH sensor nodes under both the individual and sum EH constraints when  $\sum_{k=1}^K E_k \geq E_{sum}$ .  $L = 1, 2, 3, 4$ ,  $\bar{\gamma}_{l,U} = \bar{\gamma}$  and  $\bar{\mathcal{E}}_{l,k} = \bar{\gamma}/10$ ,  $R = 3$  bps/Hz,  $E_k = 2$  and  $E_{sum} = 6$  for  $l = 1, \dots, L$  and  $k = 1, 2, 3$ .

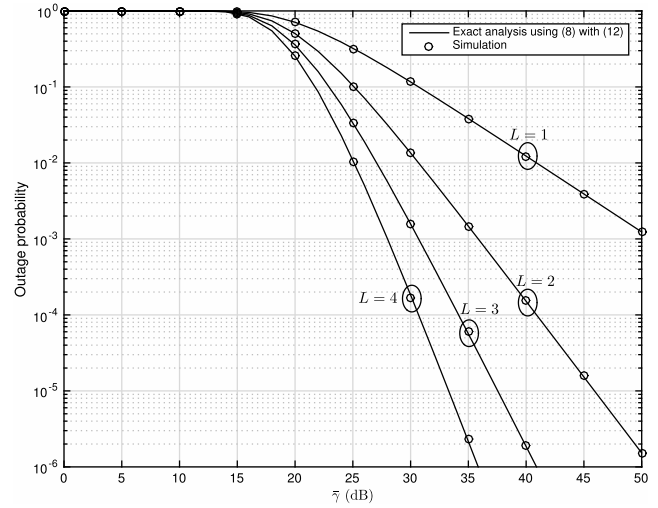


**FIGURE 3.** Rate-energy outage probability against  $\bar{\gamma}$  of the MISO system with random unitary beamforming and best beam selection in the presence of four EH sensor nodes under both the individual and sum EH constraints when  $\sum_{k=1}^K E_k < E_{sum}$  and all the average values of harvested energy  $\{\bar{\mathcal{E}}_{l,k}\}_{k=1}^K$  are distinct, i.e.,  $\bar{\mathcal{E}}_{l,i} \neq \bar{\mathcal{E}}_{l,j}$  for  $i \neq j$  with  $i, j = 1, \dots, K$ .  $L = 1, 2, 3, 4$ ,  $\bar{\gamma}_{l,U} = \bar{\gamma}$  and  $\bar{\mathcal{E}}_{l,k} = \frac{5-k}{20} \bar{\gamma}$ ,  $R = 3.5$  bps/Hz,  $E_1 = 2, E_2 = 2, E_3 = 3, E_4 = 3$ , and  $E_{sum} = 15$  for  $l = 1, \dots, L$  and  $k = 1, 2, 3, 4$ .

presence of four EH sensor nodes under both the individual and sum EH constraints when  $\sum_{k=1}^K E_k < E_{sum}$  and all the average values of harvested energy  $\{\bar{\mathcal{E}}_{l,k}\}_{k=1}^K$  are distinct, i.e.,  $\bar{\mathcal{E}}_{l,i} \neq \bar{\mathcal{E}}_{l,j}$  for  $i \neq j$  with  $i, j = 1, \dots, K$ , where we set  $L = 1, 2, 3, 4$ ,  $\bar{\gamma}_{l,U} = \bar{\gamma}$  and  $\bar{\mathcal{E}}_{l,k} = \frac{5-k}{20} \bar{\gamma}$ ,  $R = 3.5$  bps/Hz,  $E_1 = 2, E_2 = 2, E_3 = 3, E_4 = 3$ , and  $E_{sum} = 15$  for  $l = 1, \dots, L$  and  $k = 1, 2, 3, 4$ . For this case, the result is given in recursive form of (8) with (12). Fig. 4 shows the rate-energy outage probability against  $\bar{\gamma}$  of the MISO system with

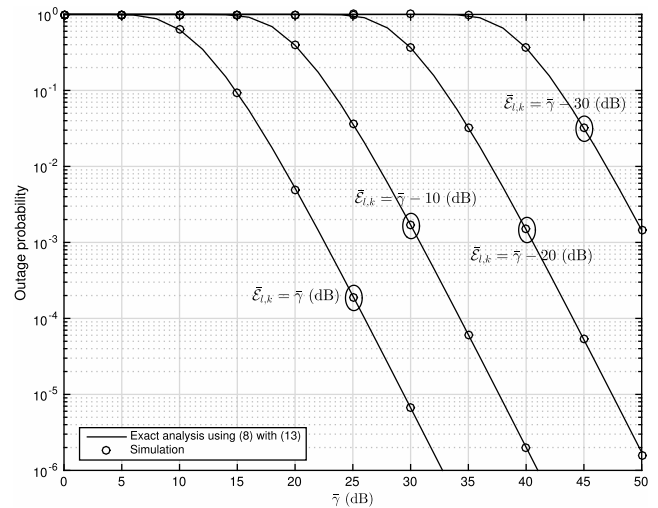


**FIGURE 4.** Rate-energy outage probability against  $\bar{\gamma}$  of the MISO system with random unitary beamforming and best beam selection in the presence of three EH sensor nodes under both the individual and sum EH constraints when  $\sum_{k=1}^K E_k < E_{sum}$  and all the average values of harvested energy are identical, i.e.,  $\bar{\mathcal{E}}_{l,k} = \bar{\mathcal{E}}_l$  for  $k = 1, \dots, K$ .  $L = 3$ ,  $\bar{\gamma}_{l,U} = \bar{\gamma}$  and  $\bar{\mathcal{E}}_{l,k} = \bar{\gamma} - m$  dB with  $m = 0, 10, 20, 30$ ,  $R = 2$  bps/Hz,  $E_1 = 3, E_2 = 4, E_3 = 5$ , and  $E_{sum} = 20$  for  $l = 1, 2, 3$  and  $k = 1, 2, 3$ .

random unitary beamforming and best beam selection in the presence of three EH sensor nodes under both the individual and sum EH constraints when  $\sum_{k=1}^K E_k < E_{sum}$  and all the average values of harvested energy are identical, i.e.,  $\bar{\mathcal{E}}_{l,k} = \bar{\mathcal{E}}_l$  for  $k = 1, \dots, K$ , where we set  $L = 3$ ,  $\bar{\gamma}_{l,U} = \bar{\gamma}$  and  $\bar{\mathcal{E}}_{l,k} = \bar{\gamma} - m$  dB with  $m = 0, 10, 20, 30$ ,  $R = 2$  bps/Hz,  $E_1 = 3, E_2 = 4, E_3 = 5$ , and  $E_{sum} = 20$  for  $l = 1, 2, 3$  and  $k = 1, 2, 3$ . For this case, the result is given in closed form of (8) with (13). Irrespective of average received power  $\bar{\gamma}$  values and/or the number of antennas at the BS and/or the number of EH sensor nodes in Figs. 2, 3, and 4, we can see that the analysis exactly matches with simulation results. Also, as the average received power  $\bar{\gamma}$  increases and/or the number  $L$  of antennas at the BS increases, we can see that the rate-energy outage performance improves.

**B. COMPARISON OF BEAM SELECTION UNDER THREE DIFFERENT EH REQUIREMENTS**

In this subsection, we check the accuracy of the obtained rate-energy outage probabilities of the MISO system when  $\sum_{k=1}^K E_k < E_{sum}$  and all the average values of harvested energy  $\{\bar{\mathcal{E}}_{l,k}\}_{k=1}^K$  are distinct under three different EH constraints: under both the individual and sum EH constraints in (8) with (12), under only the individual EH constraint in (17), and under only the sum EH constraint in (18). Fig. 5 shows three different rate-energy outage probabilities against  $\bar{\gamma}$  of beam selection for random unitary beamforming in the MISO system with three EH sensor nodes under both the individual and sum EH constraints, under only the individual EH constraint, and under only the sum EH constraint when  $\sum_{k=1}^K E_k < E_{sum}$  and all the average values of harvested

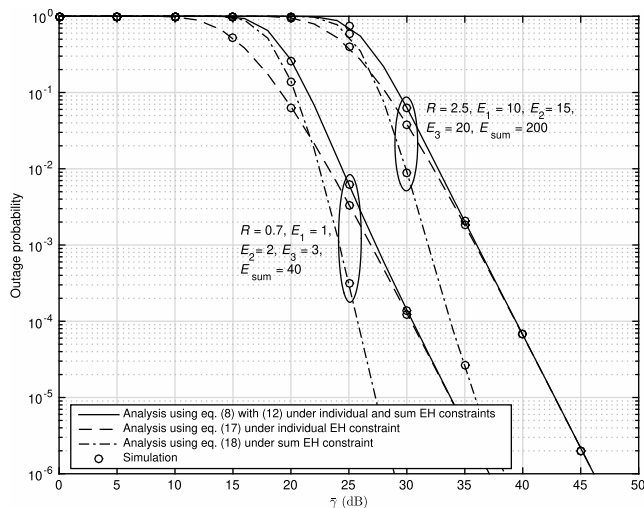


**FIGURE 5.** Rate-energy outage probability against  $\bar{\gamma}$  of beam selection for random unitary beamforming in the MISO system with three EH sensor nodes under both the individual and sum EH constraints, under only the individual EH constraint, and under only the sum EH constraint when  $\sum_{k=1}^K E_k < E_{sum}$  and all the average values of harvested energy  $\{\bar{\mathcal{E}}_{l,k}\}_{k=1}^K$  are distinct for two different systems: i)  $R = 0.7$  bps/Hz,  $E_1 = 1$ ,  $E_2 = 2$ ,  $E_3 = 3$ , and  $E_{sum} = 40$ ; and ii)  $R = 2.5$  bps/Hz,  $E_1 = 10$ ,  $E_2 = 15$ ,  $E_3 = 20$ , and  $E_{sum} = 200$ .  $L = 3$ ,  $\bar{\gamma}_{l,U} = \bar{\gamma}$  and  $\bar{\mathcal{E}}_{l,k} = \frac{5-k}{20} \bar{\gamma}$  for  $l = 1, 2, 3$  and  $k = 1, 2, 3$ .

energy  $\{\bar{\mathcal{E}}_{l,k}\}_{k=1}^K$  are distinct for two different systems: i)  $R = 0.7$  bps/Hz,  $E_1 = 1, E_2 = 2, E_3 = 3$ , and  $E_{sum} = 40$ ; and ii)  $R = 2.5$  bps/Hz,  $E_1 = 10, E_2 = 15, E_3 = 20$ , and  $E_{sum} = 200$ ,  $L = 3$ ,  $\bar{\gamma}_{l,U} = \bar{\gamma}$  and  $\bar{\mathcal{E}}_{l,k} = \frac{5-k}{20} \bar{\gamma}$  for  $l = 1, 2, 3$  and  $k = 1, 2, 3$ . Fig. 6 shows three different rate-energy outage probabilities against  $\bar{\gamma}$  of beam selection for random unitary beamforming in the MISO system with four EH sensor nodes under both the individual and sum EH constraints, under only the individual EH constraint, and under only the sum EH constraint when  $\sum_{k=1}^K E_k < E_{sum}$  and all the average values of harvested energy  $\{\bar{\mathcal{E}}_{l,k}\}_{k=1}^K$  are distinct for two different systems: i)  $R = 0.2$  bps/Hz,  $E_1 = 1, E_2 = 2, E_3 = 3, E_4 = 4$ , and  $E_{sum} = 100$ ; and ii)  $R = 5$  bps/Hz,  $E_1 = 10, E_2 = 15, E_3 = 20, E_4 = 25$ , and  $E_{sum} = 500$ ,  $L = 2$ ,  $\bar{\gamma}_{l,U} = \bar{\gamma}$  and  $\bar{\mathcal{E}}_{l,k} = \frac{5-k}{20} \bar{\gamma}$  for  $l = 1, 2$  and  $k = 1, 2, 3, 4$ . Irrespective of average received power  $\bar{\gamma}$  values in Figs. 5 and 6, we can see that the analyses exactly match with simulation results, and the rate-energy outage performance improves as the average received power  $\bar{\gamma}$  increases. In addition, we can see that the rate-energy outage probability of the MISO system under both the EH constraints is similar to that under the individual EH constraint in the high SNR regime; on the other hand, the rate-energy outage probability of the MISO system under both the EH constraints is similar to that under the sum EH constraint in the low SNR regime. The underlying reason for this can be explained as follows: as the SNR increases, the sum EH constraint can easily be satisfied with the total sum harvested energy by all the EH sensor nodes due to the averaging effect; and as the SNR decreases, the sum EH constraint becomes difficult to be satisfied.

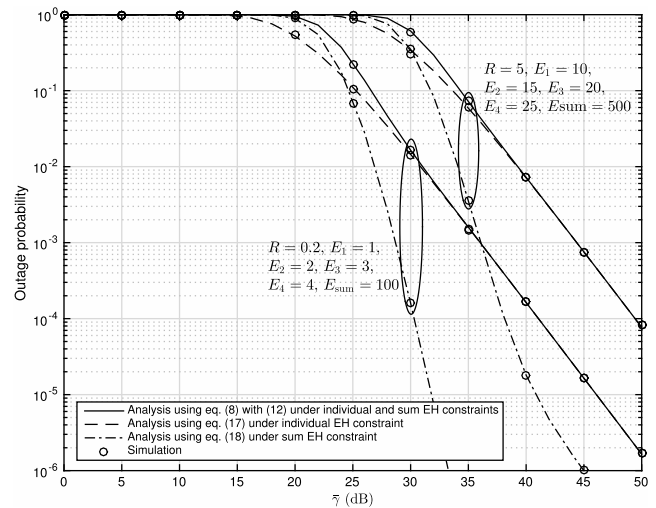


**FIGURE 6.** Rate-energy outage probability against  $\bar{\gamma}$  of beam selection for random unitary beamforming in the MISO system with four EH sensor nodes under both the individual and sum EH constraints, under only the individual EH constraint, and under only the sum EH constraint when  $\sum_{k=1}^K E_k < E_{sum}$  and all the average values of harvested energy  $\{\bar{\mathcal{E}}_{l,k}\}_{k=1}^K$  are distinct for two different systems: i)  $R = 0.2$  bps/Hz,  $E_1 = 1$ ,  $E_2 = 2$ ,  $E_3 = 3$ ,  $E_4 = 4$ , and  $E_{sum} = 100$ ; and ii)  $R = 5$  bps/Hz,  $E_1 = 10$ ,  $E_2 = 15$ ,  $E_3 = 20$ ,  $E_4 = 25$ , and  $E_{sum} = 500$ .  $L = 2$ ,  $\bar{\gamma}_{l,U} = \bar{\gamma}$  and  $\bar{\mathcal{E}}_{l,k} = \frac{5-k}{20} \bar{\gamma}$  for  $l = 1, 2$  and  $k = 1, 2, 3, 4$ .

**TABLE 1. Comparison of random unitary beamforming and conventional optimum beamforming in SWIPT.**

	random unitary beamforming	conventional optimum beamforming
number of pilot signals	$K + 1$	$K + 1$
computational complexity	low	very high
diversity order	$L$	$L$

**C. COMPARISON OF RANDOM UNITARY BEAMFORMING AND CONVENTIONAL OPTIMUM BEAMFORMING IN SWIPT**

In this subsection, we compare random unitary beamforming and conventional optimum beamforming in SWIPT in three aspects. Firstly, we consider the pilot signaling overhead of the two schemes. We assume that all the channels are reciprocal. For both schemes, the user and each sensor node broadcasts a pilot signal sequentially, and the BS receives the pilot signal and estimates the CSI, i.e.,  $h_{l,U}$  and  $h_{l,H_k}$ , for  $k = 1, \dots, K$ . Overall, the pilot signaling strategy of random unitary beamforming and conventional optimum beamforming in SWIPT are identical and the total number of required pilot signals is  $K + 1$ . We then consider the computational complexity and diversity order of the two schemes. It is well-known that the computational complexity of random unitary beamforming is very low and that of conventional optimum beamforming is generally very high; and that both random unitary beamforming and conventional optimum beamforming achieve full diversity order.

**VI. CONCLUSION**

In this paper, we have considered the MISO system consisting of a multi-antenna BS and a single-antenna user in the presence of multiple single-antenna EH sensor nodes, where the user decoded information and multiple EH sensor nodes accumulated energy through the received signals from the BS. Specifically, we have proposed beam selection of random unitary beamforming to maximize the transmission rate of the MISO system under both the individual and sum EH constraints at multiple EH sensor nodes. Then we have derived the exact rate-energy outage probability. The derived rate-energy outage expression could be used to optimize the MISO system parameters such as the number of antennas and required transmission rate at BS, and required individual/sum harvesting energy at EH sensor nodes. For future work, we will investigate some other issues with magnetic induction, practical non-linear EH models, LoS channel, and antenna correlation.

**APPENDIXES**

**APPENDIX A**

**PROOF OF THEOREM 1**

Since beams are orthonormal,  $\{\gamma_{l,U}\}_{l=1}^L$  are independent, and  $\{\mathcal{E}_{l,k}\}_{l=1}^L$  are independent, we have

$$P_{out}^{BS}(R, E) = \prod_{l=1}^L \Phi_l(R, E), \tag{A.1}$$

where

$$\Phi_l(R, E) = Pr \left[ \gamma_{l,U} < T_r \text{ or } \mathcal{E}_{l,1} < E_1 \text{ or } \dots \text{ or } \mathcal{E}_{l,K} < E_K \text{ or } \sum_{k=1}^K \mathcal{E}_{l,k} < E_{sum} \right]. \tag{A.2}$$

Note that with the selection scheme, the rate-energy outage occurs when no beam satisfies the rate and energy requirements simultaneously. Since the random variables  $\{\gamma_{l,U}, \mathcal{E}_{l,k} : l = 1, \dots, L, k = 1, \dots, K\}$  are independent one another, the probability  $\Phi_l(R, E)$  of (A.2) can be rewritten as

$$\Phi_l(R, E) = 1 - Pr[\gamma_{l,U} \geq T_r] \times Pr \left[ \mathcal{E}_{l,1} \geq E_1, \dots, \mathcal{E}_{l,K} \geq E_K, \sum_{k=1}^K \mathcal{E}_{l,k} \geq E_{sum} \right]. \tag{A.3}$$

Since the random variable  $\gamma_{l,U}$  is exponentially distributed with mean  $\bar{\gamma}_{l,U}$ , the first probability of the right-hand side of (A.3) are given in simplified form as follows:

$$Pr[\gamma_{l,U} \geq T_r] = \exp \left( -\frac{T_r}{\bar{\gamma}_{l,U}} \right). \tag{A.4}$$

Substituting (A.4) into (A.3), which in turn is substituted into (A.1), one can obtain the probability  $P_{out}^{BS}(R, E)$  of (8).

**APPENDIX B**

**PROOF OF LEMMA 2**

Since the events of  $\Upsilon_{l,K}(E_{sum}, \{E_k\}_{k=1}^K; \{\bar{\mathcal{E}}_{l,k}\}_{k=1}^K)$  in (9) are highly correlated with one another, its mathematical derivation is more challenging. We present a recursive solution as follows: we firstly consider the case when a system with one energy harvester ( $K = 1$ ); secondly the case when a system with two energy harvesters ( $K = 2$ ); and finally the case when a system with general  $K$  energy harvesters.

When  $K = 1$ , it is easy to know that  $E_{sum} = E_1$  and

$$\Upsilon_1(E_{sum}, E_1; \bar{\mathcal{E}}_{l,1}) = Pr[\mathcal{E}_{l,1} \geq E_{sum}] = \exp \left( \frac{-E_{sum}}{\bar{\mathcal{E}}_{l,1}} \right). \tag{B.1}$$

Then we consider a system with two energy harvesters ( $K = 2$ ). In this case, the probability  $\Upsilon_{l,K}(E_{sum}, \{E_k\}_{k=1}^K; \{\bar{\mathcal{E}}_{l,k}\}_{k=1}^K)$  of (9) is given by

$$\begin{aligned} \Upsilon_{l,2}(E_{sum}, \{E_k\}_{k=1}^2; \{\bar{\mathcal{E}}_{l,k}\}_{k=1}^2) &= Pr[\mathcal{E}_{l,1} \geq E_1, \mathcal{E}_{l,2} \geq E_2, \mathcal{E}_{l,1} + \mathcal{E}_{l,2} \geq E_{sum}] \\ &= Pr[\mathcal{E}_{l,2} \geq \max[E_2, E_{sum} - \mathcal{E}_{l,1}], \mathcal{E}_{l,1} \geq E_1] \\ &= Pr[\mathcal{E}_{l,2} \geq E_2, \mathcal{E}_{l,1} \geq E_{sum} - E_2, \mathcal{E}_{l,1} \geq E_1] \\ &\quad + Pr[\mathcal{E}_{l,2} \geq E_{sum} - \mathcal{E}_{l,1}, E_1 \leq \mathcal{E}_{l,1} < E_{sum} - E_2] \\ &= P_{2,1} + P_{2,2}. \end{aligned} \tag{B.2}$$



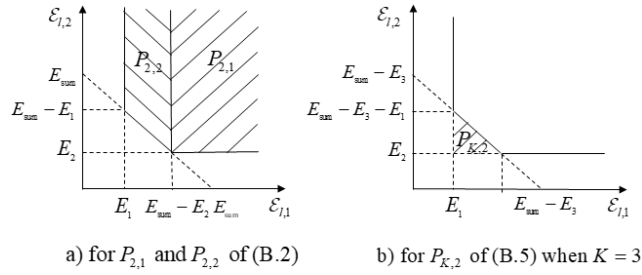


**FIGURE 7.** Integral region for  $P_{2,1}$  and  $P_{2,2}$  of (B.2) and  $P_{K,2}$  of (B.5) when  $K = 3$  in the two-dimensional region  $(\mathcal{E}_{l,1}, \mathcal{E}_{l,2})$ .

Since  $\mathcal{E}_{l,1}$  and  $\mathcal{E}_{l,2}$  are independent each other and it is obvious that  $E_{sum} - E_2 > E_1$  when  $E_1 + E_2 < E_{sum}$ , the first probability  $P_{2,1}$  of (B.2) is rewritten as

$$\begin{aligned} P_{2,1} &= \Pr[\mathcal{E}_{l,2} \geq E_2] \Pr[\mathcal{E}_{l,1} \geq \max[E_{sum} - E_2, E_1]] \\ &= \Pr[\mathcal{E}_{l,2} \geq E_2] \Pr[\mathcal{E}_{l,1} \geq E_{sum} - E_2] \\ &= \exp\left(-\frac{E_2}{\bar{\mathcal{E}}_{l,2}}\right) \Upsilon_1(E_{sum} - E_2, E_1; \bar{\mathcal{E}}_{l,1}). \end{aligned} \quad (\text{B.3})$$

Referring to Fig. 7.a, the second probability  $P_{2,2}$  of (B.2) is given by

$$\begin{aligned} P_{2,2} &= \int_{x=E_1}^{E_{sum}-E_2} \int_{x_2=E_{sum}-x_1}^{\infty} f_{\mathcal{E}_{l,1}}(x_1) f_{\mathcal{E}_{l,2}}(x_2) dx_1 dx_2 \\ &= \frac{1}{\bar{\mathcal{E}}_{l,1}} \exp\left(-\frac{E_{sum}}{\bar{\mathcal{E}}_{l,2}}\right) \int_{x_1=E_1}^{E_{sum}-E_2} \\ &\quad \times \exp\left(-x_1 \left(\frac{1}{\bar{\mathcal{E}}_{l,1}} - \frac{1}{\bar{\mathcal{E}}_{l,2}}\right)\right) dx_1 \\ &= \frac{\bar{\mathcal{E}}_{l,2}}{\bar{\mathcal{E}}_{l,2} - \bar{\mathcal{E}}_{l,1}} \exp\left(-\frac{E_{sum}}{\bar{\mathcal{E}}_{l,2}}\right) \\ &\quad \times \left[ \exp\left(-\frac{(E_{sum} - E_2)}{\bar{\mathcal{E}}_{l,1}} \left(\frac{1}{\bar{\mathcal{E}}_{l,1}} - \frac{1}{\bar{\mathcal{E}}_{l,2}}\right)\right) \right. \\ &\quad \left. - \exp\left(-\frac{E_1}{\bar{\mathcal{E}}_{l,1}} \left(\frac{1}{\bar{\mathcal{E}}_{l,1}} - \frac{1}{\bar{\mathcal{E}}_{l,2}}\right)\right) \right] \\ &= \sum_{j=1}^2 \frac{\bar{\mathcal{E}}_{l,2}}{\prod_{i=1, i \neq j}^2 (\bar{\mathcal{E}}_{l,j} - \bar{\mathcal{E}}_{l,i})} \\ &\quad \times \exp\left(-\sum_{i=1, i \neq j}^2 \frac{E_i}{\bar{\mathcal{E}}_{l,i}} - \frac{E_{sum} - \sum_{i=1, i \neq j}^2 E_i}{\bar{\mathcal{E}}_{l,j}}\right), \end{aligned} \quad (\text{B.4})$$

where  $f_X(x)$  is the probability density function (PDF) of a random variable  $X$ . Substituting (B.3) and (B.4) into (B.2) yields  $\Pr[\mathcal{E}_{l,1} \geq E_1, \mathcal{E}_{l,2} \geq E_2, \mathcal{E}_{l,1} + \mathcal{E}_{l,2} \geq E_{sum}] = \Upsilon_2(E_{sum}, E_1, E_2; \bar{\mathcal{E}}_{l,1}, \bar{\mathcal{E}}_{l,2})$ .

Finally, we consider a system with  $K$  energy harvesters and  $\sum_{k=1}^K E_k < E_{sum}$ . In this case, the probability

$\Upsilon_{l,K}(E_{sum}, \{E_k\}_{k=1}^K; \{\bar{\mathcal{E}}_{l,k}\}_{k=1}^K)$  of (9) is given by

$$\begin{aligned} &\Upsilon_{l,K}(E_{sum}, \{E_k\}_{k=1}^K; \{\bar{\mathcal{E}}_{l,k}\}_{k=1}^K) \\ &= \Pr\left[\mathcal{E}_{l,1} \geq E_1, \dots, \mathcal{E}_{l,K} \geq E_K, \sum_{k=1}^K \mathcal{E}_{l,k} \geq E_{sum}\right] \\ &= \Pr\left[\mathcal{E}_{l,K} \geq \max\left[E_K, E_{sum} - \sum_{k=1}^{K-1} \mathcal{E}_{l,k}\right], \right. \\ &\quad \left. \{\mathcal{E}_{l,k} \geq E_k\}_{k=1}^{K-1}\right] \\ &= \Pr\left[\mathcal{E}_{l,K} \geq E_K, \sum_{k=1}^{K-1} \mathcal{E}_{l,k} \geq E_{sum} - E_K, \right. \\ &\quad \left. \{\mathcal{E}_{l,k} \geq E_k\}_{k=1}^{K-1}\right] + \Pr\left[\mathcal{E}_{l,K} \geq E_{sum} - \sum_{k=1}^{K-1} \mathcal{E}_{l,k}, \right. \\ &\quad \left. \sum_{k=1}^{K-1} \mathcal{E}_{l,k} < E_{sum} - E_K, \{\mathcal{E}_{l,k} \geq E_k\}_{k=1}^{K-1}\right] \\ &= P_{K,1} + P_{K,2}. \end{aligned} \quad (\text{B.5})$$

Since  $\mathcal{E}_{l,K}$  and  $\{\mathcal{E}_{l,k}\}_{k=1}^{K-1}$  are independent one another, the probability  $P_{K,1}$  is rewritten as

$$\begin{aligned} P_{K,1} &= \Pr[\mathcal{E}_{l,K} \geq E_K] \\ &\quad \times \Pr\left[\sum_{k=1}^{K-1} \mathcal{E}_{l,k} \geq E_{sum} - E_K, \{\mathcal{E}_{l,k} \geq E_k\}_{k=1}^{K-1}\right] \\ &= \exp\left(-\frac{E_K}{\bar{\mathcal{E}}_{l,K}}\right) \\ &\quad \times \Upsilon_{K-1}(E_{sum} - E_K, \{E_k\}_{k=1}^{K-1}; \{\bar{\mathcal{E}}_{l,k}\}_{k=1}^{K-1}). \end{aligned} \quad (\text{B.6})$$

Taking a similar step to (B.4) and considering the integral region for  $\sum_{k=1}^{K-1} \mathcal{E}_{l,k} < E_{sum} - E_K$  and  $\{\mathcal{E}_{l,k} \geq E_k\}_{k=1}^{K-1}$  with a fixed  $\mathcal{E}_{l,K} = E_{sum} - \sum_{k=1}^{K-1} \mathcal{E}_{l,k}$ , one obtains (B.7), as shown at the top of the next page. Taking  $K - 2$  integrals similar to (B.4), one obtains (B.8), as shown at the top of the next page, from (B.7). Substituting (B.6) and (B.8) into (B.5) yields  $\Pr[\mathcal{E}_{l,1} \geq E_1, \mathcal{E}_{l,2} \geq E_2, \dots, \mathcal{E}_{l,K} \geq E_K, \sum_{k=1}^K \mathcal{E}_{l,k} \geq E_{sum}] = \Upsilon_{l,K}(E_{sum}, \{E_k\}_{k=1}^K; \{\bar{\mathcal{E}}_{l,k}\}_{k=1}^K)$ .

### APPENDIX C PROOF OF LEMMA 3

Taking steps similar to those used from (B.1) to (B.8) with identical average value of harvested energy  $\bar{\mathcal{E}}_l$ , it can be shown that  $P_{K,1}$  of (B.6) and  $P_{K,2}$  of (B.8) are given respectively by

$$\begin{aligned} P_{K,1} &= \exp\left(-\frac{E_K}{\bar{\mathcal{E}}_l}\right) \\ &\quad \times \Upsilon_{K-1}(E_{sum} - E_K, \{E_k\}_{k=1}^{K-1}; \{\bar{\mathcal{E}}_l\}_{k=1}^{K-1}), \end{aligned} \quad (\text{C.1})$$

$$P_{K,2} = \exp\left(-\frac{E_{sum}}{\bar{\mathcal{E}}_l}\right) \frac{(E_{sum} - \sum_{k=1}^K E_k)^{K-1}}{(K-1)! \bar{\mathcal{E}}_l}. \quad (\text{C.2})$$

Since the initial value  $\Upsilon_l(E_{sum} - E_2, E_1; \bar{\mathcal{E}}_l) = \exp\left(-\frac{(E_{sum} - E_2)}{\bar{\mathcal{E}}_l}\right)$ , one can calculate the probability

$$\begin{aligned}
 P_{K,2} &= \int_{x_1=E_1}^{E_{sum}-\sum_{k=2}^K E_k} \int_{x_2=E_2}^{E_{sum}-\sum_{k=3}^K E_k-x_1} \dots \int_{x_{K-2}=E_{K-2}}^{E_{sum}-\sum_{k=K-1}^K E_k-\sum_{k=1}^{K-3} x_k} \int_{x_{K-1}=E_{K-1}}^{E_{sum}-E_K-\sum_{k=1}^{K-2} x_k} \int_{x_K=E_{sum}-\sum_{k=1}^{K-1} x_k}^{\infty} \\
 &\quad \times \left( \prod_{k=1}^K f_{\mathcal{E}_{l,k}}(x_k) \right) dx_1 dx_2 \dots dx_{K-2} dx_{K-1} dx_K \\
 &= \frac{1}{\prod_{j=1}^{K-1} \bar{\mathcal{E}}_{l,j}} \int_{x_1=E_1}^{E_{sum}-\sum_{k=2}^K E_k} \int_{x_2=E_2}^{E_{sum}-\sum_{k=3}^K E_k-x_1} \dots \int_{x_{K-2}=E_{K-2}}^{E_{sum}-\sum_{k=K-1}^K E_k-\sum_{k=1}^{K-3} x_k} \int_{x_{K-1}=E_{K-1}}^{E_{sum}-E_K-\sum_{k=1}^{K-2} x_k} \\
 &\quad \times \exp \left( - \sum_{k=1}^{K-1} \frac{x_k}{\bar{\mathcal{E}}_{l,k}} - \frac{E_{sum}-\sum_{k=1}^{K-1} x_k}{\bar{\mathcal{E}}_{l,K}} \right) dx_1 dx_2 \dots dx_{K-2} dx_{K-1} \\
 &= \frac{\bar{\mathcal{E}}_{l,K}}{(\bar{\mathcal{E}}_{l,K}-\bar{\mathcal{E}}_{l,K-1}) \prod_{j=1}^{K-2} \bar{\mathcal{E}}_{l,j}} \int_{x_1=E_1}^{E_{sum}-\sum_{k=2}^K E_k} \int_{x_2=E_2}^{E_{sum}-\sum_{k=3}^K E_k-x_1} \dots \int_{x_{K-2}=E_{K-2}}^{E_{sum}-\sum_{k=K-1}^K E_k-\sum_{k=1}^{K-3} x_k} \\
 &\quad \times \exp \left( - \frac{E_{sum}}{\bar{\mathcal{E}}_{l,K}} - \sum_{k=1}^{K-2} x_k \left( \frac{1}{\bar{\mathcal{E}}_{l,k}} - \frac{1}{\bar{\mathcal{E}}_{l,K}} \right) \right) \left[ \exp \left( - (E_{sum}-E_K-\sum_{k=1}^{K-2} x_k) \left( \frac{1}{\bar{\mathcal{E}}_{l,K-1}} - \frac{1}{\bar{\mathcal{E}}_{l,K}} \right) \right) \right. \\
 &\quad \left. - \exp \left( - E_{K-1} \left( \frac{1}{\bar{\mathcal{E}}_{l,K-1}} - \frac{1}{\bar{\mathcal{E}}_{l,K}} \right) \right) \right] dx_1 dx_2 \dots dx_{K-2} \tag{B.7}
 \end{aligned}$$

$$= \sum_{j=1}^K \frac{\bar{\mathcal{E}}_{l,j}^{K-2} \bar{\mathcal{E}}_{l,K}}{\prod_{i=1, i \neq j}^K (\bar{\mathcal{E}}_{l,j}-\bar{\mathcal{E}}_{l,i})} \exp \left( - \sum_{i=1, i \neq j}^K \frac{E_i}{\bar{\mathcal{E}}_{l,i}} - \frac{E_{sum}-\sum_{i=1, i \neq j}^K E_i}{\bar{\mathcal{E}}_{l,j}} \right). \tag{B.8}$$

$\Upsilon_{l,K}(E_{sum}, \{E_k\}_{k=1}^K; \{\bar{\mathcal{E}}_l\}_{k=1}^K) = P_{K,1} + P_{K,2}$  in recursive way and obtains

$$\begin{aligned}
 \Upsilon_{l,K}(E_{sum}, \{E_k\}_{k=1}^K; \{\bar{\mathcal{E}}_l\}_{k=1}^K) &= \exp \left( - \frac{E_K}{\bar{\mathcal{E}}_l} \right) \\
 &\quad \times \exp \left( - \frac{E_{sum}-E_K}{\bar{\mathcal{E}}_l} \right) \sum_{m=0}^{K-2} \frac{1}{m!} \left( \frac{E_{sum}-\sum_{k=1}^K E_k}{\bar{\mathcal{E}}_l} \right)^m \\
 &\quad + \exp \left( - \frac{E_{sum}}{\bar{\mathcal{E}}_l} \right) \frac{(E_{sum}-\sum_{k=1}^K E_k)^{K-1}}{(K-1)! \bar{\mathcal{E}}_l} \\
 &= \exp \left( - \frac{E_{sum}}{\bar{\mathcal{E}}_l} \right) \sum_{m=0}^{K-1} \frac{1}{m!} \left( \frac{E_{sum}-\sum_{k=1}^K E_k}{\bar{\mathcal{E}}_l} \right)^m. \tag{C.3}
 \end{aligned}$$

Using  $\Gamma(K, x) = (K-1)! \exp(-x) \sum_{m=0}^{K-1} x^m/m!$  [36], we can derive the final expression of the probability  $\Upsilon_{l,K}(E_{sum}, \{E_k\}_{k=1}^K; \{\bar{\mathcal{E}}_l\}_{k=1}^K)$  of (C.3), which is given in (13) for general  $K$ .

REFERENCES

[1] T. Le, K. Mayaram, and T. Fiez, "Efficient far-field radio frequency energy harvesting for passively powered sensor networks," *IEEE J. Solid-State Circuits*, vol. 43, no. 5, pp. 1287–1302, May 2008.

[2] T. Paing, J. Shin, R. Zane, and Z. Popovic, "Resistor emulation approach to low-power RF energy harvesting," *IEEE Trans. Power Electron.*, vol. 23, no. 3, pp. 1494–1501, May 2008.

[3] S. Sudevalayam and P. Kulkarni, "Energy harvesting sensor nodes: Survey and implications," *IEEE Commun. Surveys Tuts.*, vol. 13, no. 3, pp. 443–461, 3rd Quart., 2011.

[4] S. Lee, R. Zhang, and K. Huang, "Opportunistic wireless energy harvesting in cognitive radio networks," *IEEE Trans. Wireless Commun.*, vol. 12, no. 9, pp. 4788–4799, Sep. 2013.

[5] D. Gunduz, K. Stamatiou, N. Michelusi, and M. Zorzi, "Designing intelligent energy harvesting communication systems," *IEEE Commun. Mag.*, vol. 52, no. 1, pp. 210–216, Jan. 2014.

[6] I. Krikidis, S. Timotheou, S. Nikolaou, G. Zheng, D. W. K. Ng, and R. Schober, "Simultaneous wireless information and power transfer in modern communication systems," *IEEE Commun. Mag.*, vol. 52, no. 11, pp. 104–110, Nov. 2014.

[7] Z. Ding, C. Zhong, D. W. K. Ng, M. Peng, H. A. Suraweera, R. Schober, and H. V. Poor, "Application of smart antenna technologies in simultaneous wireless information and power transfer," *IEEE Commun. Mag.*, vol. 53, no. 4, pp. 86–93, Apr. 2015.

[8] A. M. Fouldgar and O. Simeone, "On the transfer of information and energy in multi-user systems," *IEEE Commun. Lett.*, vol. 16, no. 11, pp. 1733–1736, Nov. 2012.

[9] R. Zhang and C. K. Ho, "MIMO broadcasting for simultaneous wireless information and power transfer," *IEEE Trans. Wireless Commun.*, vol. 12, no. 5, pp. 1989–2001, May 2013.

[10] Z. Xiang and M. Tao, "Robust beamforming for wireless information and power transmission," *IEEE Wireless Commun. Lett.*, vol. 1, no. 4, pp. 372–375, Aug. 2012.

[11] X. Zhou, R. Zhang, and C. K. Ho, "Wireless information and power transfer: Architecture design and rate-energy tradeoff," *IEEE Trans. Commun.*, vol. 61, no. 11, pp. 4754–4767, Nov. 2013.

[12] Z. Wang, Z. Chen, L. Luo, Z. Hu, and H. Liu, "Outage analysis of cognitive relay networks with energy harvesting and information transfer," in *Proc. IEEE ICC*, Sydney, NSW, Australia, Jun. 2014, pp. 4348–4353.

[13] D. Michalopoulos, H. A. Suraweera, and R. Schober, "Relay selection for simultaneous information transmission and wireless energy transfer: A tradeoff perspective," *IEEE J. Sel. Areas Commun.*, vol. 33, no. 8, pp. 1578–1594, Aug. 2015.

[14] Z. Ding, S. M. Perlaza, I. Esnaola, and H. V. Poor, "Power allocation strategies in energy harvesting wireless cooperative networks," *IEEE Trans. Wireless Commun.*, vol. 13, no. 2, pp. 846–860, Feb. 2014.

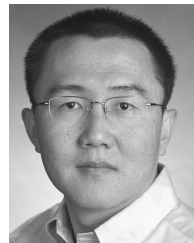
[15] A. A. Nasir, X. Zhou, S. Durrani, and R. A. Kennedy, "Relaying protocols for wireless energy harvesting and information processing," *IEEE Trans. Wireless Commun.*, vol. 12, no. 7, pp. 3622–3636, Jul. 2013.

- [16] L. Liu, R. Zhang, and K.-C. Chua, "Secrecy wireless information and power transfer with MISO beamforming," *IEEE Trans. Signal Process.*, vol. 62, no. 7, pp. 1850–1863, Apr. 2014.
- [17] J. Xu, L. Liu, and R. Zhang, "Multiuser MISO beamforming for simultaneous wireless information and power transfer," *IEEE Trans. Signal Process.*, vol. 62, no. 18, pp. 4798–4810, Sep. 2014.
- [18] C. K. Ho and R. Zhang, "Optimal energy allocation for wireless communications with energy harvesting constraints," *IEEE Trans. Signal Process.*, vol. 60, no. 9, pp. 4808–4818, Sep. 2012.
- [19] N. J. Guilar, R. Amiratharajah, and P. J. Hurst, "A full-wave rectifier with integrated peak selection for multiple electrode piezoelectric energy harvesters," *IEEE J. Solid-State Circuits*, vol. 44, no. 1, pp. 240–246, Jan. 2009.
- [20] F. Gao, T. Cui, and A. Nallanathan, "Optimal training design for channel estimation in decode-and-forward relay networks with individual and total power constraints," *IEEE Trans. Signal Process.*, vol. 56, no. 12, pp. 5937–5949, Dec. 2008.
- [21] G. Zheng, K. K. Wong, A. Paulraj, and B. Ottersten, "Collaborative-relay beamforming with perfect CSI: Optimum and distributed implementation," *IEEE Signal Process. Lett.*, vol. 16, no. 4, pp. 257–260, Apr. 2009.
- [22] G. Zheng, Y. Zhang, C. Ju, and K.-K. Wong, "A stochastic optimization approach for joint relay assignment and power allocation in orthogonal amplify-and-forward cooperative wireless networks," *IEEE Trans. Wireless Commun.*, vol. 10, no. 12, pp. 4091–4099, Dec. 2011.
- [23] Y. Zhao, R. Adve, and T. J. Lim, "Improving amplify-and-forward relay networks: Optimal power allocation versus selection," in *Proc. IEEE ISIT*, Seattle, WA, USA, Jul. 2006, pp. 1234–1238.
- [24] Z. Wang, Z. Chen, L. Luo, Z. Hu, and H. Liu, "Optimum multi-hop transmission strategies for energy constrained wireless sensor networks," in *Proc. IEEE ICC*, Ottawa, ON, Canada, Jun. 2012, pp. 260–264.
- [25] B. Hassibi and T. L. Marzetta, "Multiple-antennas and isotropically random unitary inputs: The received signal density in closed form," *IEEE Trans. Inf. Theory*, vol. 48, no. 6, pp. 1473–1484, Jun. 2002.
- [26] J. Chung, C.-S. Hwang, K. Kim, and Y. K. Kim, "A random beamforming technique in MIMO systems exploiting multiuser diversity," *IEEE J. Sel. Areas Commun.*, vol. 21, no. 5, pp. 848–855, Jun. 2003.
- [27] M. Sharif and B. Hassibi, "On the capacity of MIMO broadcast channels with partial side information," *IEEE Trans. Inf. Theory*, vol. 51, no. 2, pp. 506–522, Feb. 2005.
- [28] H.-C. Yang, P. Lu, H.-K. Sung, and Y.-C. Ko, "Exact sum-rate analysis of MIMO broadcast channels with random unitary beamforming," *IEEE Trans. Commun.*, vol. 59, no. 11, pp. 2982–2986, Nov. 2011.
- [29] T. Wu and H. C. Yang, "RF energy harvesting with cooperative beam selection for wireless sensors," *IEEE Wireless Commun. Lett.*, vol. 3, no. 6, pp. 585–588, Dec. 2014.
- [30] T. Wu, H.-C. Yang, and Y.-C. Liang, "Cooperative secondary beam selection for cognitive multiuser MIMO transmission with random beamforming," *IEEE Trans. Cogn. Commun. Netw.*, vol. 2, no. 2, pp. 141–149, Jun. 2016.
- [31] W. Han, J. Ge, and J. Men, "Performance analysis for NOMA energy harvesting relaying networks with transmit antenna selection and maximal-ratio combining over Nakagami- $m$  fading," *IET Commun.*, vol. 10, no. 18, pp. 2687–2693, Dec. 2016.
- [32] J. Ye, H. Lei, Y. Liu, G. Pan, D. B. Costa, Q. Ni, and Z. Ding, "Cooperative communications with wireless energy harvesting over Nakagami- $m$  fading channels," *IEEE Trans. Commun.*, vol. 65, no. 12, pp. 5149–5164, Dec. 2017.
- [33] I. Orikumhi, C. Y. Leow, and Z. Ding, "Wireless information and power transfer in MIMO virtual full duplex relaying system," *IEEE Trans. Veh. Technol.*, vol. 66, no. 12, pp. 11001–11010, Dec. 2017.
- [34] C. Xu, M. Zheng, W. Liang, H. Yu, and Y. Liang, "End-to-end throughput maximization for underlay multi-hop cognitive radio networks with RF energy harvesting," *IEEE Trans. Wireless Commun.*, vol. 16, no. 6, pp. 3561–3572, Jun. 2017.
- [35] D. Tse and P. Viswanath, *Fundamentals Wireless Communications*. Cambridge, MA, USA: Cambridge Univ. Press, 2005.
- [36] I. S. Gradshteyn and I. M. Ryzhik, *Table of Integrals, Series and Products*, 6th ed. San Diego, CA, USA: Academic, 2000.
- [37] A. Bletsas, H. Shin, and M. Z. Win, "Cooperative communications with outage-optimal opportunistic relaying," *IEEE Trans. Wireless Commun.*, vol. 6, no. 9, pp. 3450–3460, Sep. 2007.



**MINCHUL JU** (M'12) received the B.S. degree in electrical engineering from the Pohang University of Science and Technology (POSTECH), Pohang, South Korea, in 1997, the M.S. degree in electrical engineering from the Korea Advanced Institute of Science and Technology (KAIST), Daejeon, South Korea, in 1999, and the Ph.D. degree in electrical and computer engineering from Queen's University, ON, Canada, in 2010. From 1999 to 2005, he was a Researcher with the Korea Electronics

Technology Institute (KETI), South Korea, where he was involved in many projects related with WPAN systems, such as Bluetooth, IEEE802.15.3, and IEEE802.11. Since September 2011, he has been with the School of Electrical Engineering, Kookmin University, Seoul, South Korea, where he is currently an Associate Professor. His research interests include the areas of drone communications, cooperative networks, and energy harvesting.



**HONG-CHUAN YANG** (S'00–M'03–SM'07) received the Ph.D. degree in electrical engineering from the University of Minnesota, Minneapolis, USA, in 2003. Since September 2003, he has been with the Department of Electrical and Computer Engineering, University of Victoria, Victoria, BC, Canada, where he is currently a Professor. From 1995 to 1998, he was a Research Associate with the Science and Technology Information Center (STIC), Ministry of Posts and Telecomm (MPT), Beijing, China. He has published over 200 referred journals and conference papers. He is also the author of *Introduction of Digital Wireless Communications* by IET Press and the coauthor of *Order Statistics in Wireless Communications* by Cambridge University Press. His current research focuses on the design and analysis of wireless transmission technologies for the advanced Internet of Things.

• • •